

Experimental Investigation of Splashing Behaviour on Dry Solid Surfaces under High Parameters

S. Frohwein, T. Eisfeld^{*}, F. Joos
Power Engineering/Laboratory of Turbomachinery
Helmut-Schmidt-University
University of the Federal Armed Forces Hamburg
Holstenhofweg 85 - D-22043 Hamburg, Germany

Abstract

The subject matter of the experimental investigation in this study is the impact of dry solid surfaces on the behaviour of droplets. Different surfaces with partially deterministic and stochastic roughness have been used as impact targets. The experiments were performed under high splashing parameters. A shadowgraphy system was used to measure the characteristics of the primary and the secondary droplets.

The results presented in this study show the dependence of the break-up process on rough surfaces. Furthermore, the study investigated the influence of the primary droplet velocity and the primary droplet diameter on the characteristics of the secondary droplets. The quantitative results are illustrated as distributions; these were compared according to different statistical parameters. The results show, if the surface roughness has the same dimension as the diameter of the primary droplet, then there is an increased number of secondary droplets after the impact of this primary droplet. In addition to this, it turns out that the primary droplet diameter and its velocity have different effects on the characteristics of the secondary droplets. It became apparent that the primary droplet diameter affects the number of secondary droplets and the primary droplet velocity affects the secondary droplet velocity.

Introduction

The phenomenon of drop impingement onto solid surfaces occurs in several technical applications - for instance: fuel injection, blade erosion in steam turbines, or spray cooling. There is a great interest in understanding the different manifestations of the drop impact. The difficulty is the prediction of the outcome. Diverse physical phenomena such as forces effects - due to surface tension or inertia are interacting at the same time. Because of the complexity of this hardly calculable process, many studies are pertaining to drop impact [1-11].

A subject, which is considered in the research of wet-compression in gas turbines, is droplet-blade interaction in connection with two-phase flows in turbomachinery [6, 10]. In this context, an increasingly discussed issue for applications in turbomachinery is inlet fogging. Additionally, detailed information about droplet behaviour in accelerating flows are available [12].

Often, one objective of numerical and experimental investigations is to find out the thresholds of the different outcomes of drop impact onto solid surfaces - like splashing or deposition [7, 9, 11]. As in this study, an experimental investigation about impact behaviour of droplets within an parameter range as described in [6] has not been considered before. Investigations about impact behaviour of droplets on different surfaces are operating in a much lower parameter range [1, 3, 9]. The purpose of this study was to model impact conditions as they are relevant in turbomachinery [6].

Materials and Methods

The setup used to generate droplets and to observe the droplet impact is illustrated in Figure 1. Free falling droplets with a constant diameter were investigated by dripping off a cannula. Predominantly the droplet diameter depends on the diameter of the cannula [13]. The relative velocity of the surrounding air to the droplet is adjusted by a compressed air supply. The drops fall through a light barrier that sends a TTL- signal to a measuring board. The signal activates the CCD camera (2048 x 2048 pixels, frame rate 8 Hz) and the background illumination with a previously defined time delay. While changing the time delay, it is possible to show the different phases of the drop impact process. Furthermore, the camera is able to take two separate exposures within a time increment down to 1 μs in different frames, as shown in Figure 2. Using this double frame mode enables the software to calculate the velocity of the primary and secondary droplets. The lowest possible time increment and time delay allowed by the camera is 1 μs . This configuration option allows reproducible outcomes.

^{*}Corresponding author: eisfeld@hsu-hh.de

The objective was to capture the characteristics of the primary and secondary droplets. There are many parameters, which have an influence on the impact behaviour like the primary droplet velocity, the surface tension of the used liquid, or the surface roughness of the impact target [9].

In [9] it is shown that the droplet impact behaviour depends generally on the Reynolds number,

$$Re_d = \frac{\rho_d \cdot d_d \cdot v_d}{\mu_d} \quad (1)$$

the Weber number,

$$We = \frac{v_d^2 \cdot d_d \cdot \rho_d}{\sigma_d} \quad (2)$$

and the non-dimensional surface roughness

$$\gamma = \frac{2 \cdot R_T}{d_d}. \quad (3)$$

Also the Ohnesorge number is important to describe the ratio of the capillarity to the viscosity time scale.

$$Oh = \frac{\sqrt{We}}{Re_d} = \frac{\mu_d}{\sqrt{\rho_d \cdot d_d \cdot \sigma_d}} \quad (4)$$

In connection to this, the droplet-on-surface interactions are classified by the K-factor.

$$K = Oh \cdot Re_d^{1.25} = \left(\frac{\rho_d^3 \cdot d_d^3 \cdot v_d^5}{\sigma_d^2 \cdot \mu_d} \right)^{0.25} \quad (5)$$

This characteristic fragmentation parameter describes the occurrence of secondary droplets [9, 10]; it is essential for this experimental investigation.

The experiments were subdivided into two parts. One part of the measurements was executed with different droplet diameters. In the other part, the K-factor was changed by accelerating the droplets using the compressed air supply. The parameters are given in Table 1. All experiments were performed under environmental conditions (temperature 293 K, pressure 1013 kPa). The used liquid was water; the characteristics are given in Table 2.

Series of measurement	D_{pr} [mm]	K [–]
1	6	835
		725
		600
2	4	441
	4.6	490
	6	521

Table 1. Parameters used for the Experiments

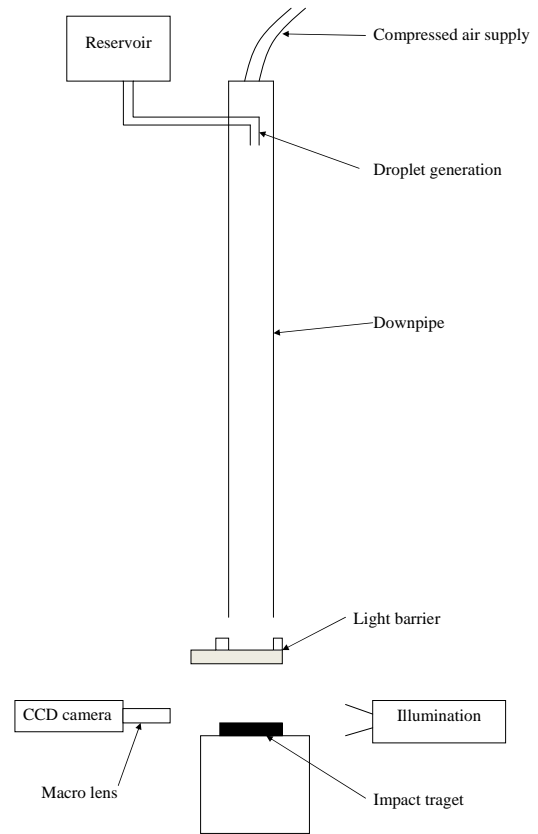


Figure 1. Experimental Setup

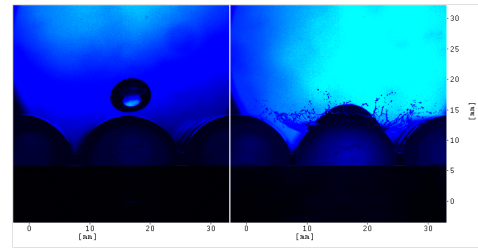


Figure 2. Double Frame Recording of a splashing droplet ($\tau = 1$ ms)

	ρ_d [kg/m ³]	σ_d [N/m]	μ_d [Pa/s]
Water	1000	0.07275	0.001

Table 2. Characteristics of the used liquid

	Material	D_{pr} [mm]	R_t [μ m]
sphere min.	Steel	5	12.95
sphere max.	Natron glass	16	4.95

Table 3. Characteristics of the used surfaces

Spheres were used to model the surfaces roughness of the compressor blades. The diameters of these spheres were confirming to the values for the non-dimensional surfaces roughness γ given in [6, 9]. They describe the maximum and the minimum of the non-dimensional surface roughness [6]. A couple of spheres, side by side, constitute a partial deterministic surface - only partial because the roughness of the spheres itself is not negligible.

Shadowgraphy is the optical method with which the measurements were made. This method allows to measure the velocity and the size of particles down to $20 \mu\text{m}$. The measurement area in the setup illustrated in Figure 1 has a size of approximately $28 \text{ mm} \times 16.5 \text{ mm}$. Using the macro lens in combination with the camera makes it possible to reach such a large area without losing definition. A detailed description of the shadowgraphy system is given in [10].

Results and Discussion

The drop impact process with a K-factor, which is corresponding approximately to the conditions in a transonic compressor ($v_d = 290 \text{ m/s}$, $d_d = 10 \mu\text{m}$) [6], is shown in Figure 3. Because the K-factor exceeds the Splashing-threshold ($K = 57.7$) [9], the typical characteristics of the secondary droplet generation are discernible [7]. The first picture in Figure 3 shows the primary droplet 2 ms before the impact. Because of high We-numbers, the accelerated droplet is deformed. This complanate shape is caused by the interaction between the drop's surface tension and the air resistance. The images 3 up to 5 depict the splashing mechanism of the primary droplet onto a surface that is equal to highest surfaces roughness of the compressor blades ($\gamma = 6$) as described in [6]. The characteristics of the mechanism become evident: the propagating free crown-like liquid sheet, the free rim at its top, the cups formed because of the disturbance of the rim, the thin jets emerging at cups and the secondary droplets formed by the capillary break-up [7].

Forces due to surfaces tension, viscosity, and inertia determine the whole process in general [1, 7]. Furthermore, the roughness of the surface has an effect on the impact behaviour. Figure 4 shows the drop impact on a surface that is equal to the lowest surfaces roughness of the described blades ($\gamma = 1.88$) under the same conditions as shown in Figure 3. In this case, the droplet break-up is completely chaotic and essentially different to the behaviour shown in Figure 3. This is not surprising since the roughness height shown in Figure 3 is more than two times higher than the droplet diameter. The droplet diameter shown in Figure 4 is about the same dimension as the surface roughness, this supports the droplet breakup [9]. To give a general statement about the droplet distributions and to quantify the results, 500 pictures per experiment were taken in the moment of splashing. Besides, the break-up process can be divided in two phases.

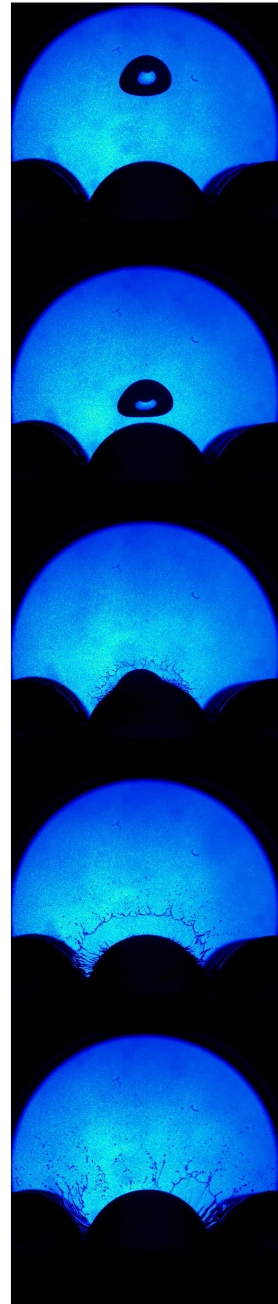


Figure 3. Drop impact with $\gamma = 6$, $K = 600$, $We = 2062$, $Oh = 1.53 \cdot 10^{-3}$

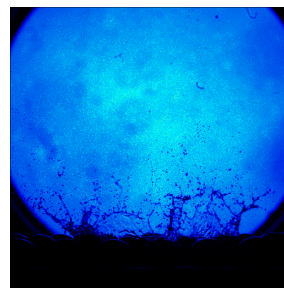


Figure 4. Drop impact with $\gamma = 1.88$, $K = 600$, $We = 2062$, $Oh = 1.53 \cdot 10^{-3}$

During the first phase secondary droplets with small diameters (in relation to all generated droplets) were generated. During the second phase droplets with bigger diameters were generated [11]. The highest feasible K-factor with this setup is $K = 835$, which is corresponding to a primary droplet diameter of $10.7 \mu\text{m}$ measured during the experiments in a transonic compressor [6].

The distribution of the primary droplets, created during the experiment with $K = 835$, is illustrated in Figure 5. The droplets are normal distributed with a confidence level of 99%, the average diameter is 5.3 mm with a standard deviation of 0.2 mm . Despite the small variations of the standard deviation in the average diameter, the distributions of the primary droplets were similar to the one shown in Figure 5 - during all experiments.

One measure for the degree of primary droplet deformation is the ratio of the minimum and maximum primary droplet diameter. Due to a constant effect of the air resistance and the gravity, a diameter oscillation could not be observed. For example the average diameter ratio of the primary droplets measured during the experiment with $K=600$, 2 ms before the impact amounts 0.745 with a standard deviation of 0.05. The value 1 ms before the impact amounts 0.726 with a standard deviation of 0.04. Comparable results were established during other measurements under similar conditions. A considerable amount of oscillation is not observed.

In the first series of measurements, the variable parameter was the K-factor; the values are listed in Table 1. The distribution of the secondary droplet diameters that are triggered by the initial drop impact on a surface with the lowest and the highest roughness height (with $K = 835$) are compared in Figure 6. The run of the distributions is alike.

The ratio of the average diameter of the secondary droplets and the primary droplet diameter caused by the high surface roughness is 0.031 related to the primary droplet diameter with a standard deviation of 48.8 %; the value caused by the lower surface roughness is 0.029, including a standard deviation of 42.2 %. The related average velocity of the secondary droplets are 4.2 with a standard deviation of 44.7 % (high roughness) and 3.8 with a standard deviation of 43.9 % (low roughness). The high values of the standard deviation show that the characteristic velocity of the secondary droplets is fluctuating in a wide range. In comparison, the number of emerging droplets is more significant; on average 88 droplets per recorded image with high roughness and 216 with low roughness. This verifies the statement that a roughness height with the same dimension as the primary droplet diameter supports the droplet break-up [9].

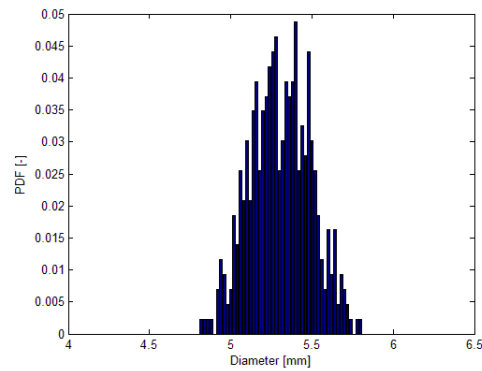


Figure 5. Probability density function of the primary droplets $K = 835$

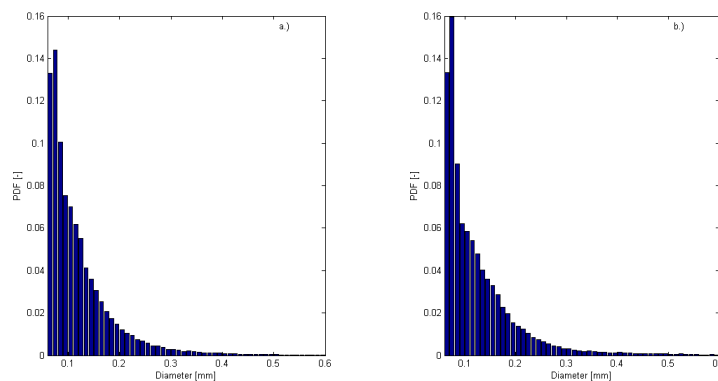


Figure 6. Probability density function of the secondary droplets with $K = 835$, a.) $\gamma = 6$ b.) $\gamma = 1.88$

Figure 7 shows the same comparison as Figure 6, just that $K = 600$. It is clearly visible that the differences between the distributions and in comparison to Figure 6 are marginal. The value for the average diameter of the secondary droplets caused by the high surface roughness diversify only 0.4% ($d = 0.155 \text{ mm}$) and the average

diameter caused by the low surface roughness only 1.4% ($d = 0.149$ mm). Almost the same holds true for the standard deviation. An analogous conclusion may be drawn comparing the other experiments. It is obvious that the influence of the K-factor on the secondary droplet diameter in this index area of minor significance. Considerably more interesting is the development of the velocity. In comparison to the velocity in the experiment where $K = 835$, here the velocity of the primary droplets was reduced by 21.5%, which results in a secondary droplet velocity of about 51% to 57% respectively (depending on the surface's roughness). This leads to the assumption, that the connection between the primary droplet velocity and the secondary droplet velocity is exponential. In theory, the

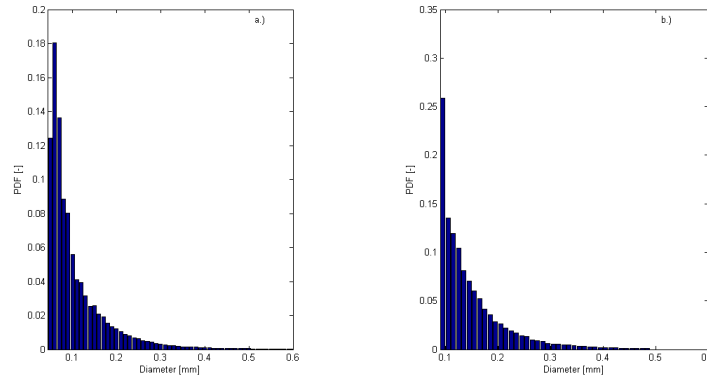


Figure 7. Probability density function of the secondary droplets with $K = 600$, a.) $\gamma = 6$ b.) $\gamma = 1.88$

secondary droplets are able to reach sonic velocity of water, but the kinetic energy of the primary droplet is largely dissipated by the viscosity of the liquid during the deformation [9].

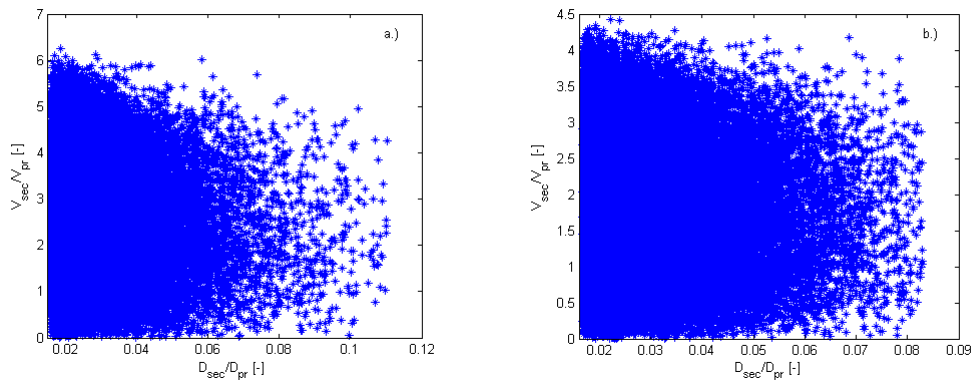


Figure 8. Normalised velocity-diameter diagram of the secondary droplets, $\gamma = 1.88$, a.) $K = 835$, b.) $K = 600$

Figure 8 shows the normalised velocity-diameter diagram of the experiments where $K = 835$ and $K = 600$ - performed with the low surface roughness. The diameter and velocity values were scaled by the average values of the primary droplets. This creates a relative error of 3.5% ($K = 835$) and 1.3% ($K = 600$) respectively for the diameter values. The relative error of the velocity values is 1.8% ($K = 835$) and 0.6% ($K = 600$) respectively. The velocity-diameter diagram summarizes the essential information about the characteristics of the secondary droplets for when the splashing parameters were changed. In addition to this, all values of the velocity are represented for each individual diameter, only the number of values is altering.

Further uncertainties arise from the fact that the measurement is a two-dimensional projection of the problem. Moreover, the background illumination decides on the smallest detectable droplet diameter.

The second series of measurements was an investigation about the influence of the primary droplet diameter on the impact behaviour. While executing the experiments with different diameters (listed in Table 1), the primary droplet velocity was kept constant (5 m/s). A comparison of the different surfaces confirms the result, which was

established during the experiments with a varied K-factor. In addition to this, the number of secondary droplets increases exponentially with the primary droplet diameter. For instance, the experiment with the low surface roughness and a primary droplet diameter of 5.5 mm results in 129 secondary droplets (when impacting) per recorded image. The same experiment with a 20% decreased primary droplet diameter causes the emergence of 52 droplets per recorded image after the impact. The reason for this is the changed volume of the primary droplet and its related changed kinetic energy [9]. The K-factor has an effect on the kinetic energy as well, because the diameter and the velocity are employed in the equation of the K-factor. However, such a correlation between the primary droplet velocity and the number of secondary droplets could not be observed (during the experiments with a varied K-factor). The explanation for that could be the fact that the primary droplet diameter and consequently the primary droplet volume was kept constant (Table 1) keeping the amount of initial material constant. This makes a crucial difference to the experiments with the varied primary droplet diameter. Nevertheless, the impact of the variation of the primary droplet diameter on the secondary droplet distribution depicted in Figure 9 is marginal, which has also been found in the first test series. Additionally, the effect of the K-factor variation by diameter on the velocity-diameter distributions (Figure 10) is different to the effect of variation by primary droplet velocity (Figure 8). Comparing these distributions, it can be seen that an increased primary droplet diameter yields increased secondary droplet diameters whereas an increased primary droplet velocity yields higher secondary droplet velocities.

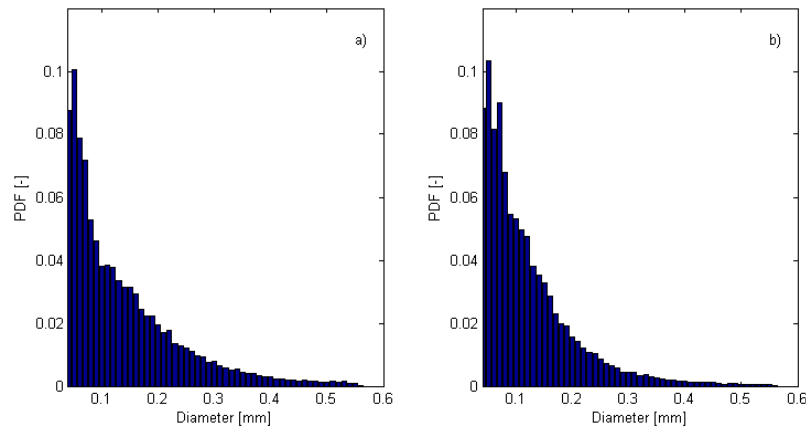


Figure 9. Probability density function of the secondary droplets with $\gamma = 1.88$ a.) $D_{pr} = 4$ mm b.) $D_{pr} = 6$ mm

In theory, the secondary droplets are able to reach sonic velocity of water, but the kinetic energy of the primary droplet is largely dissipated by the viscosity of the liquid during the deformation [9].

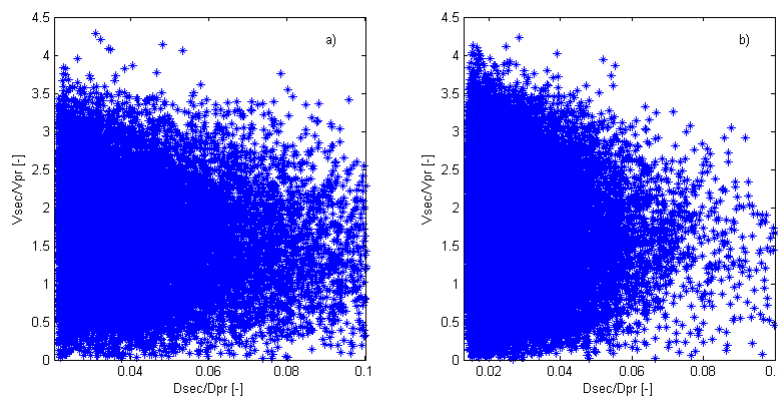


Figure 10. Normalised velocity-diameter diagram of the secondary droplets, $\gamma = 1.88$, a.) $D_{pr} = 4$ mm b.) $D_{pr} = 6$ mm

Conclusion

A detailed knowledge about the characteristics of secondary droplets caused by splashing is essential for the correct application in turbomachinery. However, reliable models for the impact behaviour of droplets, which are influenced by high splashing parameters, are still not available.

Therefore, experimental investigations of a single drop impact in an parameter range according to the conditions in a transonic compressor were performed. To increase the predictability of the outcome, the number, the size and the velocity of the secondary droplets were measured and analysed. The results show a strong dependence on the surface roughness of the surfaces. Under these conditions a lower surface roughness leads to finer distributions. Furthermore, different effects of the changed primary droplet velocity and the primary droplet diameter could be observed. The results show that a variation of velocity affects the velocity of the secondary droplets and a varied diameter affects the number of secondary droplets.

In order to increase the quantifiability of the outcome, future investigations should use a three-dimensional measuring system.

Acknowledgements

The authors would like to thank the DFG for supporting this research.

Nomenclature

d_d	Droplet diameter	CCD	Charged Couple Device
D_{pr}	Primary droplet diameter	TTL	Transistor-transistor logic
D_{sec}	Secondary droplet diameter	PDF	Probability density function
R_t	Surfaces roughness height		
v_d	Droplet velocity	γ	Non-dimensional surfaces roughness
		μ_d	Dynamic viscosity of the liquid
K	Splashing parameter	ρ_d	Density of the liquid
Oh	Ohnesorge number	σ_d	Droplet surface tension
Re_d	Droplet material Reynolds number	τ	Time increment
We	Weber number		

References

- [1] Geldron, W.I., Rioboo, R., Jakirlic, S., Muzaferija, S., and Tropea, C., *International Conference on Liquid Atomization and Spray Systems*, Pasadena, CA, USA, July 2000, pp.1175-1180
- [2] Roisman, I.V., and Tropea, C., *International Conference on Liquid Atomization and Spray Systems*, Zurich, Switzerland, September 2001, pp.657-662
- [3] Rioboo, R., Roisman, I.V., and Tropea, C., *International Conference on Liquid Atomization and Spray Systems*, Zurich, Switzerland, September 2001, pp.837-842
- [4] Cossali, G.E., Marengo, M., and Santini, M., *International Conference on Liquid Atomization and Spray Systems*, Nottingham, England, September 2004, p.79
- [5] Kalantari, D., and Tropea, C., *International Conference on Liquid Atomization and Spray Systems*, Orleans, France, September 2005, pp.413-418
- [6] Eisfeld, T., and Joos, F., *ASME Turbo Expo*, Orlando, USA, June 2009, GT2009-59365
- [7] Yarin, A.L., *Annual Review of Fluid Mechanics* 38:159-192 (2006)
- [8] Roisman, I.V., Horvat, K., and Tropea, C., *Physics of Fluids* 18:102104 (2006)
- [9] Mundo, C., "Zur Sekundaerzerstaebung newtonscher Fluide an Oberflaechen", University of Erlangen-Nuernberg, 1996
- [10] Ulrichs, E.S., "Experimental investigations into the behaviour and influence of water droplets in a compressor cascade flow", University of the Federal Armed Forces Hamburg, 2007
- [11] Urban, J., "Numerische Untersuchung und Modellierung von Tropfen Wand Interaktionen", University of Stuttgart, 2009
- [12] Schmelz, F., "Tropfenzerfall in beschleunigten Gasstroemungen", University of Dortmund, 2002
- [13] Reske, R., "Experimentelle Untersuchungen des Verhaltens frei fallender Wassertropfen beim Auftreffen auf duennen Wandfilmen", progress report VDI No. 115, 1987
- [14] Wiegand, H., "Die Einwirkung eines ebenen Stroemungsfeldes auf frei bewegliche Tropfen und ihren Widerstandsbeiwert im Reynoldszahlenbereich von 50 bis 2000", progress report VDI No. 120, 1987